MANCHESTER 1824
The University of Manchester

The University of Manchester Research

High Power Broadband Graphene Non-Foster Circuit Enabled Class-J GaN HEMT Power Amplifier

DOI:
10.1002/mop.31427

Document Version
Accepted author manuscript

Link to publication record in Manchester Research Explorer

Citation for published version (APA):
Akwuruoha, C. N., & Hu, Z. (2018). High Power Broadband Graphene Non-Foster Circuit Enabled Class-J GaN HEMT Power Amplifier. *Microwave and Optical Technology Letters*. https://doi.org/10.1002/mop.31427

Published in:
Microwave and Optical Technology Letters

Citing this paper
Please note that where the full-text provided on Manchester Research Explorer is the Author Accepted Manuscript or Proof version this may differ from the final Published version. If citing, it is advised that you check and use the publisher's definitive version.

General rights
Copyright and moral rights for the publications made accessible in the Research Explorer are retained by the authors and/or other copyright owners and it is a condition of accessing publications that users recognise and abide by the legal requirements associated with these rights.

Takedown policy
If you believe that this document breaches copyright please refer to the University of Manchester’s Takedown Procedures [http://man.ac.uk/04Y6Bo] or contact uml.scholarlycommunications@manchester.ac.uk providing relevant details, so we can investigate your claim.

Download date:04. Nov. 2024

High Power Broadband Graphene Non-Foster Circuit Enabled Class-J GaN HEMT Power Amplifier

Charles Nwakanma Akwuruoha *, Zhirun Hu

School of Electrical and Electronic Engineering, The University of Manchester, Manchester, United Kingdom
*charlesnwakanma.akwuruoha@manchester.ac.uk

Abstract: This paper presents high power broadband graphene non-Foster circuit (NFC) enabled Class-J GaN HEMT power amplifier (PA). A graphene resonant tunneling diode (RTD) NFC is proposed to provide negative differential resistance characteristics and to create an effective negative capacitance. The NFC is integrated in the input matching network of the Class-J GaN HEMT PA to cancel out the transistor input parasitic capacitance so as to enhance PA bandwidth, efficiency, output power and gain. The PA design is based on Cree's packaged GaN HEMT CGHV40030F biased with drain supply voltage of 50V at quiescent drain-to-source current of 44 mA. The PA operates from 3.4 to 4.0 GHz with center frequency of 3.7 GHz. The effective negative capacitance of the NFC from 3.4 to 4.0 GHz stands at -3.3 to -6.0 pF. An effective capacitance of -3.7 pF has been obtained at 3.7 GHz. The PA has small signal gain of 16.1 dB at 3.7 GHz. Large signal simulation input power sweep from 1 to 33 dBm at 3.7 GHz, indicates that the PA has 57.8 % drain efficiency, 54.7 % power added efficiency (PAE), 44.6 dBm (28.8W) output power and 11.6 dB transducer power gain at input power of 33 dBm.

1. Introduction

Graphene has become one of the emerging materials for many applications in microwave, millimeter wave and terahertz frequencies since its discovery [1]-[4]. Graphene is a zero-band gap two-dimensional material with excellent electrical properties that have been exploited in field effect transistors (GFETs) [5]-[7], tunable attenuator [8] , inkjet-printed resistors [9] and graphene resonant tunneling diode (RTD) [10]-[13]. In this paper, Class-J GaN HEMT PA with non-Foster circuit (NFC) made of RTD is proposed. The graphene RTD is simulated using small signal equivalent circuit [14]-[18]. The RTD is subsequently used in the design of the graphene NFC. The graphene NFC functions as negative impedance inverter which provides the effective negative capacitance required to cancel out the transistor input parasitic capacitance. NFC can be classified either as negative impedance converter (NIC) or negative impedance inverter (NII) [19]-[20] and characterized by deliberately violating Foster theorem [21] such that the reflection coefficient direction on a Smith chart is counter-clockwise with respect to frequency while having negative reactance/susceptance. NFCs have reportedly been used to enhance antenna bandwidth [19], [22]-[24]. In power amplifiers, NFCs have been reportedly used for: bandwidth enhancement of Doherty PA [25], interstage matching network to miniaturize the size of GaN pHEMT PA [26] and gain enhancement of distributed PA [27]. In all these works, the NFCs were realized using traditional transistor circuit which rather increases the complexity of the PA circuit and makes realization difficult. On the other hand, a simple negative resistance network can be used to realize an NII [28]. In this paper graphene RTD is proposed for the implementation of the NII which provides the negative capacitance required to enhance the efficiency, output power, gain and bandwidth of the Class-J PA. The proposed graphene NFC PA will find application in transmitters with high power broadband capabilities for the proposed 5G low frequency applications [29]. This paper is structured as follows. Section II discusses Class-J PA theory. Section III presents NFC theory and the graphene NFC design. Section IV provides graphene NFC PA design and analysis of the simulation results. Section V concludes the work.

2. Class-J power amplifier theory

The Class-J mode is usually biased as Class-B or deep Class AB PA whereby the transistor functions as a current generator such that the RF current waveform is a half-wave rectified sinewave [30]-[35]. The matching network is low pass filter structures aimed at blocking all components of harmonics than the fundamental. Therefore, the transistor current (I_Q) regarding the half-wave rectified sinewave is given by [30]

$$I_Q = I_{pk}\sin\psi \qquad 0<\psi<\pi \qquad (1)$$
$$= 0 \qquad \pi<\psi<2\pi$$

where ψ is the conduction angle and I_{pk} is the peak value of the half-wave rectified output current sine waveform. The output current and voltage are half-wave rectified sine waves with phase overlap and are 45° out of phase [31].

Since the effect of transistor output capacitance on the fundamental is mitigated by applying a reactive termination at the fundamental load thereby changing it from resistive to reactive regime, the DC drain supply current is given by

$$I_{dc} = \frac{I_{pk}}{\pi} \qquad (2)$$

The other higher order even harmonics than second harmonic are non-existent while third harmonic components of impedance is assumed to be shorted out [32].

The first and second harmonic components of the impedance denoted respectively by Z_{f0} and Z_{2f0} are related to the optimum load resistance R_{opt} and given by [31]

$$Z_{fo} = R_{opt} + j * R_{opt} \qquad (3)$$

$$Z_{2fo} = 0 - j * \frac{3\pi}{8} * R_{opt} \qquad (4)$$

$$R_{opt} = \frac{V_{dc}-V_{knee}}{I_{pk}/2} \quad (5)$$

where V_{dc} and V_{knee} are the drain supply and knee voltages respectively.

3. Resonant Tunneling Diode

Resonant tunneling diode (RTD) is a form of tunneling diode that finds applications in electronic and communication circuits where there is desirability to enhance switching speed [36-[37]. The basic theory, operation and applications of RTD can be found in [36]-[40]. The energy band diagram of RTD [37] showing movement of electrons as well as the conduction band (E_c), valence band (E_b) and fermi level (E_f) in the n and p regions is shown in Fig. 1

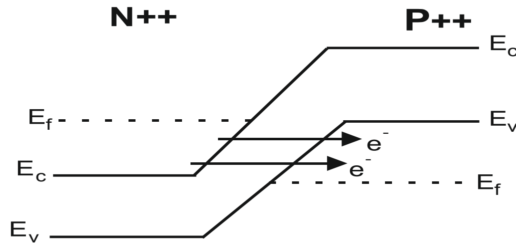

Fig. 1. Energy band diagram of RTD

4. NFC theory and Graphene NFC design

4.1. NFC Theory

NFC has negative reactance slope across its operational frequency such that the derivatives of reactance (X) and susceptance (B) with angular frequency (ω) is given by [41]

$$\frac{dX}{d\omega} < 0 \quad and \quad \frac{dB}{d\omega} < 0 \quad (6)$$

NFC is classified as open circuit stable or short circuit stable (balanced or unbalanced) [42]. In balanced NFC, there is non-Foster behavior at the two ports. The balanced NFC is also referred to as floating NFC. In unbalanced NFC, non-Foster property is obtained at only one port as the other port is shorted. In this work, balanced NFC is proposed.

4.2. Graphene RTD NFC Design

The proposed graphene RTD NFC consists of monolayer graphene RTD, inductor and resistors. The graphene RTD NFC functions as NII. In view of the fact that negative resistance circuit placed in series with other elements in a circuit with inductive load will result in negative capacitance NFC while the one placed in a circuit with capacitive load will result in negative inductance NFC [17], a negative capacitance NFC is proposed in this work. The equivalent circuit model of the proposed graphene RTD has similar schematic to the GaAs RTD reported in [18]. There are two stages involved in the design of the graphene RTD NFC in this work. The first stage proposes the design of a small signal equivalent circuit model. In the second stage, the graphene RTD equivalent circuit model was used to design the graphene RTD NFC. Different implementations of graphene RTD have been reported in [10]-[13]. The graphene RTD equivalent model proposed in this work was based on the device reported in [13]. The graphene RTD has negative differential resistance (NDR) characteristic from DC bias voltage of 1.7 to 3.0 V as shown in Fig. 2. In this work, the negative differential resistance (R_{dif}) used in the design of the graphene NFC was -25Ω. The resistance (-25Ω) was calculated from the RTD I-V characteristics shown in Fig. 2 by

$$R_{dif} = \Delta V/\Delta I = (V_2-V_1) / (I_2-I_1) \quad (7)$$

The -25Ω was introduced into the graphene NFC schematic and simulated with the aid of equations in Keysight's Advanced Design System (ADS) software [43]. The graphene NFC schematic circuit is shown in Fig. 3. The magnitude and imaginary part of input impedance (Z_{in}) characteristics obtained from the graphene NFC simulation is shown in Fig. 4. The result indicates that the NFC has effective negative capacitance which ranges from -3.3 to -6.0 pF from 3.4 to 4 GHz. The effective negative capacitance at 3.7 GHz stands at -3.7 pF as shown in Fig. 5.

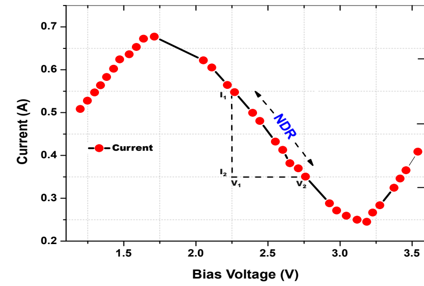

Fig. 2. RTD negative resistance

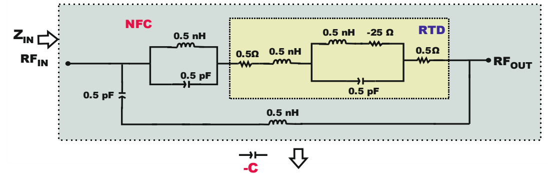

Fig. 3. Graphene NFC schematic circuit

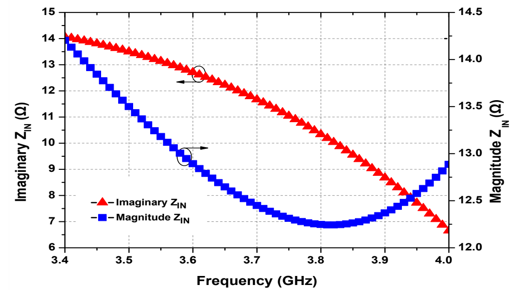

Fig. 4. Magnitude and Imaginary parts of input impedance

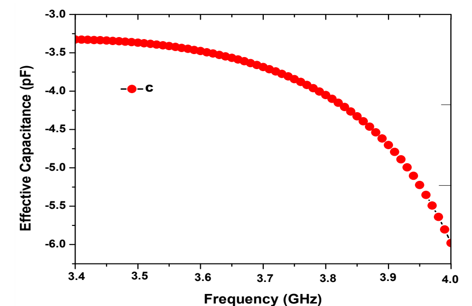

Fig. 5. NFC Effective negative capacitance

5. PA design, Simulation result and Discussion

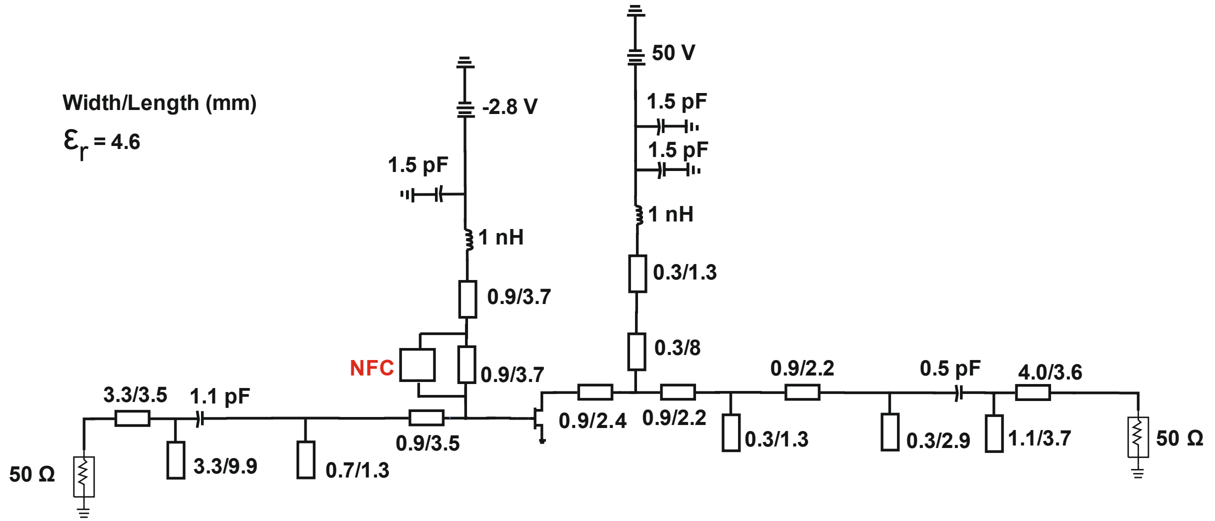

Fig. 6. PA schematic circuit

5.1. PA Design

The PA shown in Fig. 6 was designed based on Cree's CGHV40030F packaged GaN HEMT biased with drain supply voltage of 50 V at quiescent drain-to-source (I_{DSq}) current of 44mA. The power transistor biasing here is aimed at ensuring half-wave rectified output current and voltage sine waveforms. The DC I-V characteristics bias points are shown in Fig. 7. Harmonic source and load pull simulations were carried out to determine the source and load impedances respectively required to synthesize the input and output matching networks for maximum output power. The graphene NFC forms part of the input matching network and was placed at the gate of the power transistor to provide the negative capacitance required to cancel out the input parasitic capacitance of the transistor. The PA circuit consists of distributed transmission lines used to implement the input/output matching networks as well as lumped capacitors and inductors. The lumped components in the circuit functions as DC feed inductors, DC blocking capacitors and by-pass capacitors respectively. The quarter-wave transmission lines and stubs have dimensions shown as width/length (mm). The input and output matching networks were both matched to 50 Ω source and load impedance respectively.

5.2. Small Signal Simulation Results and Discussion

Small signal S-parameter simulation was carried on the PA from 3.4 to 4.0 GHz with center frequency at 3.7 GHz. The result are shown in Fig. 8,indicating that the PA has S_{21} of 16.1 dB, S_{11} of -7.5 dB, S_{22} of -7.5 dB and S_{12} of -35 dB. In view of the inherent oscillations associated with NFC which could affect the stability of the PA, the PA was subjected to two steps of stability check namely: the K-test and Nyquist criterion. The Rollet's K-factor [44] shown in Fig. 9, indicates that the PA is unconditionally stable. The PA was further subjected to Nyquist criterion to determine if there were some hidden oscillations or instability. The PA was also found to be stable as the S_{11} in the Nyquist plot did not encircle the origin as would have been the case if the PA was unstable [17]. The Nyquist plot is shown in Fig. 10.

5.3. Large Signal Simulation Results and Discussion

One-tone harmonic balance simulation was carried out on the PA from 3.4 to 4.0 GHz at center frequency of 3.7 GHz. The simulation was carried out by sweeping the input power from 1 to 33 dBm at center frequency of 3.7 GHz. The result shows that the PA has linear performance. The linear performance was obtained for such performance indicators as: output power, drain efficiency, PAE and transducer power gain. The PA recorded peak values of drain efficiency, PAE, output power and transducer power gain at 33 dBm input power. The result also indicates that at center frequency of 3.7 GHz, the PA has 57.8% drain efficiency, 54.7% PAE, 44.6 dBm (28.8W) and 11.6 dB power gain as shown in Figs. 11 and 12. The comparison of the performance of the proposed NFC PA with other published NFC PAs is shown in Table. 1.

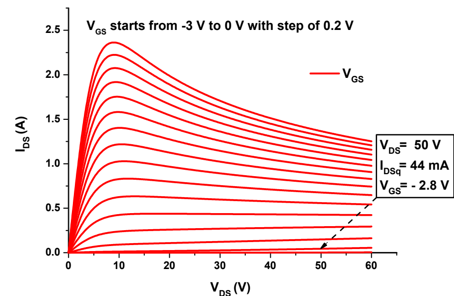

Fig. 7. I-V Characteristics DC bias points

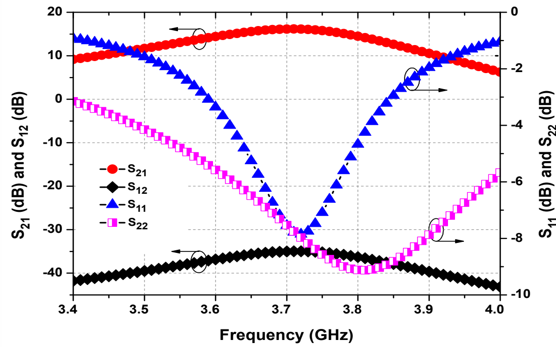

Fig. 8. *S-Parameters*

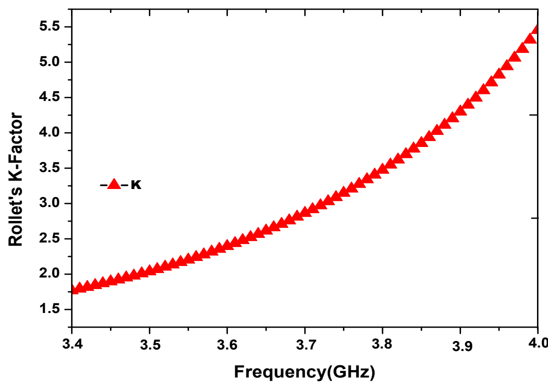

Fig. 9. *Rollet's K-Factor*

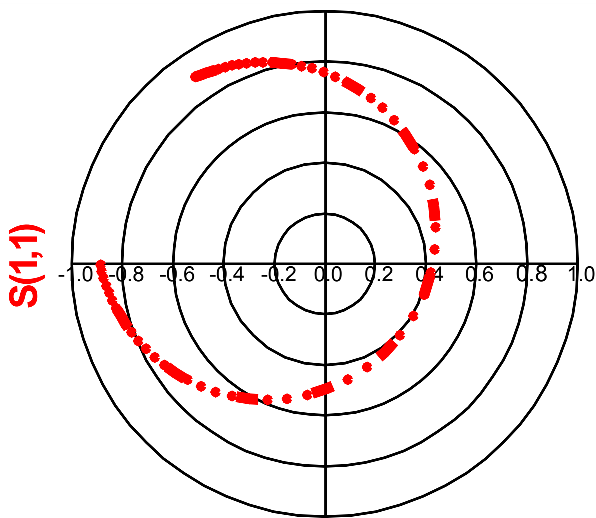

Fig. 10. *Nyquist Stability Criterion for PA stability from 3.4 to 4.0 GHz*

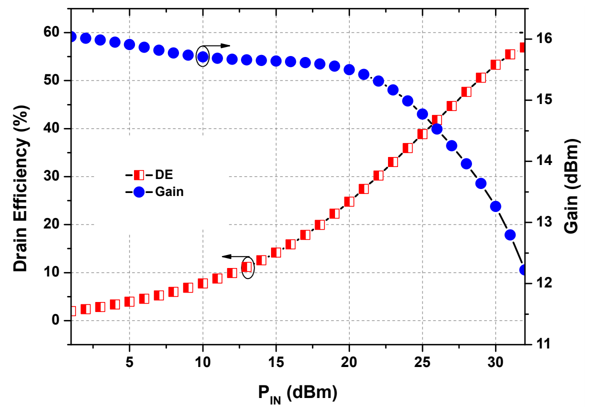

Fig. 11. *Drain Efficiency and Power Gain*

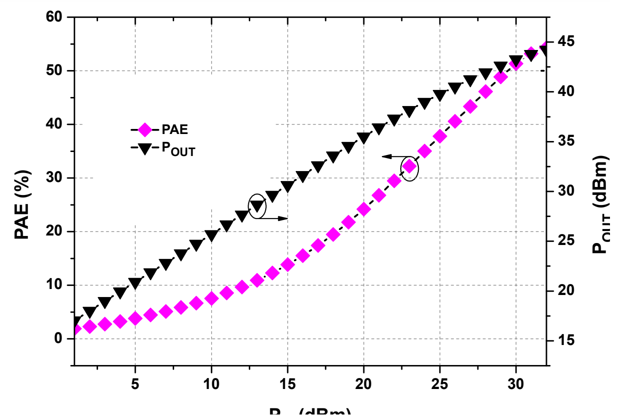

Fig. 12. *PAE and output power*

Table 1 Comparison of proposed PA with other published NFC PAs.

Reference No.	Frequency (GHz)	Efficiency (%)	Output power (dBm)
[25]	1.9-2.2	68	30
[26]	6-18	21	37.5
[27]	0-29.4	-	21
[This work]	3.4-4.0	57.8	44.6

6. Conclusion

A graphene NFC Class-J GaN HEMT power amplifier, have been proposed, designed and simulated. The simulation results indicate that graphene NFC can be added to the input matching network of the PA to cancel out transistor input parasitic capacitance at microwave frequencies. This work indicates that the use of RTD in the design of graphene RTD in the NFC is an effective method of reducing the complexity of the NFC design. The broadband graphene NFC Class-J PA will find applications in high power broadband applications. This also underscores the need for possible exploitation of graphene circuits and components in Class-J GaN HEMT PA design.

7. Acknowledgment

The first author is grateful to tertiary education trust fund Nigeria for sponsoring his PhD. The authors are thankful to Cree Incorporations for providing the model used in this work.

Reference

[1] A. K. Geim and K. S. Novoselov, “ The rise of graphene,” Nature Materials 6, pp.183-191, 2007.

[2] A. H. Castro, F. Guinea, N. M. R. Peres, K. S. Novoselov and A.K. Gein, “The electronic properties of graphene,” Reviews of modern physics, Vol. 81, No. 1, pp. 109-162, March 2009.

[3] M. Bozzi, L. Pierantoni and S. Belluci, “Applications of Graphene at Microwave Frequencies,” Radioengineering, Vol. 24, No. 3, pp. 661-669, Sept. 2015.

[4] J. S. Gomez-Diaz and J. Perruisseau-Carrier, “Microwave to THz Properties of Graphene and Potential Antenna Applications,” Proceedings of ISAP2012, Nagoya, Japan, pp. 239-242, 2012.

[5] M.C. Lemme, T. J. Echtermeyer, Mathias Baus, and Heinrich Kurz, “ A Graphene Field-Effect Device,” IEEE Electron Device Letters, Vol. 28, No. 4, pp. 282-284, April 2007.

[6] J. Zhu and J. C. S. Woo, “A Novel Graphene Channel Field Effect Transistor with Schottky Tunneling Source and Drain,” 37th European Solid State Device Research Conference, Germany,pp.243-246, Sept 2007.

[7] X. Yang, G. Liu, A. A. Balandin, and K. Mohanram, “Triple-Mode Single-Transistor Graphene Amplifier and Its Applications,” American Chemical Society (ACS) Nano 4 (10) , pp. 5532-5538, 2010.

[8] R. Sordan, A. C. Ferrari, “Gigahertz Multi-Transistor Graphene-based Electronically Tuneable Microstrip Attenuator,” Nano-material nano technology 4:18, pp. 1-6, 2014.

[9] M. Michael, C. Biswas and A. B. Kaul, “High-performance ink-jet printed graphene resistors formed with environmentallyfriendly surfactant-free inks for extreme thermal environments,” Elsevier Applied materials today, pp. 16-21, 2017.

[10] A. Y. Goharrizi, M. Zoghi and M. Saremi, “Armchair Graphene Nanoribbon Resonant Tunneling Diodes Using Antidote and BN Doping,” IEEE Trans. on Electron Devices, vol. 63, no. 9, pp. 3761-3768, Sep., 2016.

[11] J. Gaskell, L. Eaves, K. S. Novoselov, A. Mishchenko, A. K. Geim, T. M. Fromhold and M. T. Greenway, “Graphene-hexagonal boron nitride resonant tunneling diodes as high-frequency oscillators,” Appl. Phys. Lett. 107, pp. 103105-1 – 103105- 4, 2015.

[12] V. H. Nguyen, F. Mazzamuto, A. Bournel and P. Dollfus, “Resonant tunnelling diodes based on graphene/h-BN heterostructure,” J. Phys. D: Appl. Phys. 45, 325104, pp. 1-4, 2012.

[13] V. Nam Do and P. Dollfus, “Negative differential resistance in zigzag-edge graphene nanoribbon junctions,” J. Appl. Phys. 063705-1 – 063705-5, 2010.

[14] R. E. Miles, G. Millington, R. D. Pollard, D. P. Steenson, J. M. Chamberlain and M. Henin, “Accurate Equivalent Circuit based on Resonant Tunneling Diodes,” Electronic letters, vol. 27. no. 5, pp. 427-428, Feb., 1991.

[15] Q. Liu, A Seabaugh, P. Chahal and F. J. Morris, “Unified AC Model for the Resonant Tunneling Diode,” IEEE Trans. on Electron Devices, vol. 51, no. 5, pp. 653-657, May 2004.

[16] J. M. Gering, D. A. Crim, D. G. Morgan, P. D. Coleman, W. Klopp and H. Morkoc, “A small-signal equivalent circuit model for GaAs-AlxGa1-xAs resonant tunneling heterostructures at microwave frequencies,” Journal of Applied Physics, 61(1),pp. 271-276, Jan. 1987.

[17] D. S. Nagarkoti, Y. Hoo, D. P. Steenson, L. Li, E. H. Linfield and K. Z. Rajab “Design of Broadband Non-Foster Circuits Based on Resonant Tunneling Diodes,” IEEE Antennas and Wireless Letters, vol. 15, 2016.

[18] Kwaspen, J. J. M.; Lepsa, M. I.; van der Roer, T. G.; Vleuten, van der, W. C. “Accurate equivalent–network modelling of GaAs/AlAs based resonant tunneling diodes with thin barrier layers,” Elecctronic Letters, 33(19), pp. 1657-1658, 1997.

[19] A. M. Elfrgani and R. G. Rojas, “Successful Realization of Non-Foster circuit for wideband antenna applications,” IEEE MTTS-S Int. Microw. Symp. Dig., pp. 1-4, 2015.

[20] W. R. Lundry, “Negative Impedance Circuits-Some Basic Relations and Limitations,” IRE Trans. Circuit Theory, vol CT-4, pp. 132-139, Sep. 1957.

[21] R. M. Foster, “A reactance theorem,” Bell System technical journal, vol. 3, no. 2, pp. 259-267, Nov. 1924.

[22] S. E. Sussman –Fort, “Matching Network Design Using Non-Foster Impedance impedances,” Int. Jornal of RF and Microwave Computer-Aided Engineering, Wiley periodicals, Inc., pp. 135-142, 2006.

[23] D. S. Nagarkoti, K. Z. Rajab and Y. Hao, “Design and Stability of Negative Impedance Circuits for Non-Foster Matching of a Monopole Antenna”, The 8th European Conference on Antennas and Propagation, pp. 2707- 2709, 2014.

[24] H. Mirzaei and G. V. Eleftheriades, “A Wideband Metamaterial-Inspired Compact Antenna Using Embedded Non-Foster Matching” IEEE Int. Symp. on Antennas and Propagation, pp. 1950-1953, 2011.

[25] L. M. Ledezma, “Doherty power amplifier with Lumped non-Foster impedance inverter,” in IEEE WMCS Symp., pp. 1-4, 2015.

[26] S. Lee, H. Park, J. Kim, and Y. Kwon, “A 6-18 GHz GaN pHEMT Power Amplifier Using Non-Foster Matching,” IEEE MTT-S Int. Microw. Symp. Dig., pp. 1-4, 2015.

[27] A. Ghadiri, and K. Moez, "Gain-Enhanced Distributed Amplifier Using Negative Capacitance", IEEE Trans. Circuits and Sys., vol. 57, no. 11, pp. 2834-2843, June 2010.
[28] K. L. Su, "A Mehod for Realizing the Negative-Impedance Inverter," IEEE Journal of Solid State Circuits, Vol. Sc-2, no. 1, pp. 22-25, March 1967.
[29] Ofcom, " Update on 5G spectrum in the UK," Ofcom publication, pp. 1-19, February 8, 2017.
[30] S. C. Cripps, "RF Power Amplifier for Wireless Communications," Artech House Inc. , Boston, 2nd edn., 2006, pp. 67-76.
[31] S. Rezaei, L. Belostotski, F. M. Ghannouchi and P. Aflaki, "Integrated Design of a Class-J Power Amplifier," IEEE Trans. on microw. theory and tech., vol. 61, no. 4, pp. 1639-1648, April 2013.
[32] P. Wright, J. Lees, J. Benedikt, P. J. Tasker, and S, C. Cripps, " A Methodology for Realizing High Efficiency Class-J in a Linear and Broadband PA," IEEE Trans. on microw. Theory and tech., vol. 57, no. 12, pp. 3196-3204, Dec. 2009.
[33] C. M. Anderson et al., "Theory and Design of Class-J power Amplifier With Dynamic Load Modulation," IEEE Trans. on microw. theory and tech., vol. 60, no. 12, pp. 3778-3786, Dec. 2012.
[34] A. Jain, P. R. Hannurkar, S. K. Pathak, D. K. Shama and A. K. Gupta, "Investigation of class J continuous mode for high –power solid state RF amplifier," IET microw. antennas propag., vol. 7, iss. 8, pp. 686-692, 2013.
[35] S. park, J. Woo, U. Kim and Y. Kwon, "Braodband CMOS Stacked RF Power Amplifier Using Reconfigurable Interstage Network for Wideband Envelope Tracking," IEEE Trans. on microw. theory tech., vol. 60, no. 8, pp. 2562-2570, 2012.
[36] J. P. Sun, G. I. Haddad, "Resonant Tunneling Diodes: Models and Properties," Proc. IEEE , vol. 86, no. 4, pp. 641-661, April 1998.
[37] T. Akeyoshi, H. Matsuzaki, T. Itoh, T. Waho, J. Osaka and M. Yamamoto, "Applications of Resonant-Tunneling Diodes to High-Speed Digital ICs," 11th Int. conf. on Indium Phosphide and Related materials, Davos, Switzerland, pp. 405-410, May 1999.
[38] J. M. Longras Figueiredo, C. N. Ironside and C. R. Stanley," Electric field swiching in a resonant tunneling diode electroabsorption modulator," IEEE J. Quantum Electronics, vol. 37, no. 12, pp. 101-107, Dec. 2001.
[39] K. Asakawa, M. Naoi, Y. Iki, M. Shinada, and M. Suhara, "Equivalent circuit modeling of triple-barrier resonant tunneling diodes taking nonlinear quantum inductance and capacitance into account," Phys. Status Solidi C7, no. 10, pp. 2555-2558, 2010.
[40] E. R. Brown, J. R. Soderstrom, C. D. Parker, L. J. Mahoney, K. M. Molvar and T.C McGill, "Oscillations up to 712 GHz in InAs/AlSb resonant-tunneling diodes," Appl. Phys. Lett. 58 (20), pp. 2291-2293, May 1991.
[41] A. A. Muller and S. Lucyszyn, "Properties of purely reactive Foster and non-Foster passive networks," electronic letters, vol. 51, no. 23, pp. 1882-1884, Nov. 2015.
[42] J. G. Linvill, " Transistor Negative –Impedance Converters," Proceedings of the I.R.E, pp. 725-729, 1953.
[43] ADS, "Using Simulator Expressions in Advanced Design System," ADS 2008 documentation.
[44] R. W. Jackson, "Rollet Proviso in the Stability of Linear Microwave Circuits-A Tutorial," IEEE Trans. on Microw. Theory and Tech., vol. 54, no. 3, pp. 993-1000, March 2006.